Structural and magnetic properties of CuSb2O6 probed by ESR

Monika Heinrich, Hans-Albrecht Krug von Nidda, Alexander Krimmel, Alois Loidl, R. M. Eremina, A. D. Ineev, B. I. Kochelaev, A. V. Prokofiev, W. Assmus

Angaben zur Veröffentlichung / Publication details:

Heinrich, Monika, Hans-Albrecht Krug von Nidda, Alexander Krimmel, Alois Loidl, R. M. Eremina, A. D. Ineev, B. I. Kochelaev, A. V. Prokofiev, and W. Assmus. 2003. "Structural and magnetic properties of CuSb2O6 probed by ESR." *Physical Review B* 67 (22): 224418. https://doi.org/10.1103/PhysRevB.67.224418.

Structural and magnetic properties of $CuSb_2O_6$ probed by ESR

M. Heinrich,[1] H.-A. Krug von Nidda,[1] A. Krimmel,[1] A. Loidl,[1] R. M. Eremina,[2,1] A. D. Ineev,[3] B. I. Kochelaev,[3,1] A. V. Prokofiev,[4,5] and W. Assmus[4]

[1]*Experimentalphysik V, Elektronische Korrelationen und Magnetismus, Institut für Physik, Universität Augsburg, D-86135 Augsburg, Germany*

[2]*E. K. Zavoisky Physical-Technical Institute, 420029 Kazan, Russia*

[3]*Department of Physics, Kazan State University, 420008 Kazan, Russia*

[4]*Physikalisches Institut, Johann-Wolfgang-Goethe-Universität, D-60054 Frankfurt, Germany*

[5]*A. F. Ioffe Physical Technical Institute, 194021 St. Petersburg, Russia*

(Received 22 November 2002; published 16 June 2003)

A detailed electron-spin-resonance (ESR) investigation is performed in the one-dimensional magnet $CuSb_2O_6$ on both single crystals and polycrystals. Angular-dependent ESR data on the single crystal are interpreted in terms of the anisotropic Zeeman interaction due to the Jahn-Teller distortion of the two inequivalent CuO_6 octahedra. The very strong increase of the ESR linewidth with increasing temperature on approaching the monoclinic-to-tetragonal phase transition at about 400 K indicates the thermal activation of a dynamic Jahn-Teller process. Utilizing temperature-dependent x-ray diffraction experiments we propose the monoclinic angle β as the order parameter of this phase transition.

DOI: 10.1103/PhysRevB.67.224418 PACS number(s): 76.30.Fc, 71.70.Ej, 73.90.+f

I. INTRODUCTION

The discovery of a spin-Peierls transition in the one-dimensional (1D) Heisenberg antiferromagnet $CuGeO_3$ (Ref. 1) in 1993 entailed an intensive search for other inorganic spin-Peierls systems. This renewed the investigations of transition-metal oxides with spin $S=1/2$ ions such as Cu^{2+}. For $CuSb_2O_6$ the strong decrease of the susceptibility below 9 K was discussed controversially. Nakua and Greedan[2] claimed long-range magnetic order at low temperature using neutron powder diffraction, whereas NMR measurements were first interpreted in terms of a spin-Peierls transition by Kato *et al.*[3] Meanwhile, additional susceptibility measurements on single crystals clarified this question[4] and unambiguously verified long-range antiferromagnetic ordering below 8.6 K. Recent NMR and neutron diffraction experiments yield the same result.[5] However, $CuSb_2O_6$ exhibits peculiar lattice and magnetic properties which deserve a detailed study.

In the high-temperature modification ($T>380$ K) $CuSb_2O_6$ crystallizes in the ideal tetragonal trirutile structure. The elementary cell of the trirutile structure is shown in Fig. 1. It can be generated from the rutile structure by tripling the c axis and possesses a regular distribution of divalent and pentavalent cations, consisting of a network of edge and corner sharing CuO_6 and SbO_6 octahedra. Along the c axis the magnetic Cu^{2+} ions are separated from each other by two sheets of diamagnetic ions.[6] Below 380 K a second-order phase transition from tetragonal α-$CuSb_2O_6$ (space group $P4_2/nmn$) to monoclinic β-$CuSb_2O_6$ (space group $P2_1/n$) takes place,[7,8] whereby the equivalence of the four O2 oxygen atoms is lifted in the low-temperature phase.[6] While the crystal structure indicates a nearly square planar Cu^{2+} lattice at the c-axis coordinates 0 and $c/2$ as in other trirutiles, in this compound a Cu-O-O-Cu superexchange pathway along the [110] direction is dominant, giving rise to 1D magnetic chains.[2] Theoretical investigations[9] confirm that the magnetic chains in one layer run along the $(a+b)$ direction, in the other layer in the $(a-b)$ direction. Along these directions the equatorial CuO_4 units are arranged coplanar and have the shortest intermonomer O-O distance.

Previously, Giere *et al.*[8] investigated polycrystalline samples of $CuSb_2O_6$ by different methods. They discovered that the CuO_6 octahedra switch from an elongated (β-$CuSb_2O_6$) shape to a compressed (α-$CuSb_2O_6$) shape at

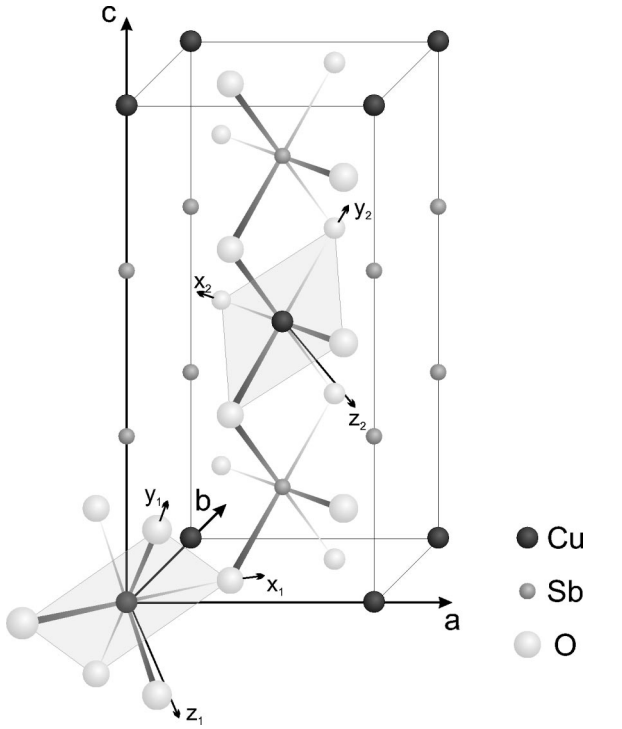

FIG. 1. The trirutile structure. x_i (O1), y_i (O2), and z_i (O2a), where $i=1,2$, indicate the local coordinate systems (oxygen positions) of the two inequivalent oxygen octahedra of the unit cell. The shaded areas denote the equatorial planes of the octahedra.

the phase transition at 380 K, but the directions of elongation and compression are not the same. In contrast the Sb-O distances change only slightly when passing through the phase transition. In the low-temperature modification the direction of elongation is along the O2a-Cu bonds with an angle of about 12° with respect to the normal vector of the equatorial plane of the short Cu-O spacings. For both magnetically inequivalent CuO_6 octahedra this equatorial plane is sketched in Fig. 1. The radial distortion parameter $\rho = 2(\delta a_x^2 + \delta a_y^2 + \delta a_z^2)^{1/2}$ is $\cong 13$ pm for the CuO_6 polyhedra in β-$CuSb_2O_6$, where the δa_i $(i = x,y,z)$ denote the deviations of the Cu-O bond lengths from the averaged spacing. Optical spectroscopy[8] yields a ^2E_g ground-state splitting $\Delta E = 2150\ \mathrm{cm}^{-1} = 3100$ K. The phase transition of $CuSb_2O_6$ at about 400 K can be understood as a thermally induced averaging process between two possible elongation directions of the oxygen octahedra. Below the transition the lowest vibronic states are localized in two energy minima of the ground-state potential surface, which correspond to octahedra elongated along the Cu-O2a bond or the Cu-O2 bond (static Jahn-Teller effect), respectively. Above 400 K higher vibronic states are occupied, leading to a fast dynamic exchange between the two energy minima of the different elongation possibilities and result in an averaged compressed structure (dynamic Jahn-Teller effect).

Here we present a detailed electron-spin-resonance (ESR) study of $CuSb_2O_6$ accompanied by x-ray and magnetization measurements. ESR is well suited to investigate the microscopic properties of this compound, because it directly probes the Cu ion, which is responsible for both the magnetic properties and the Jahn-Teller distortion of the lattice. From the anisotropy of the magnetic resonance we will obtain information on the local geometry and interactions of the CuO_6 octahedra. We will see that the temperature dependence of the ESR signal is very sensitive to the transition from the static into the dynamic Jahn-Teller phase.

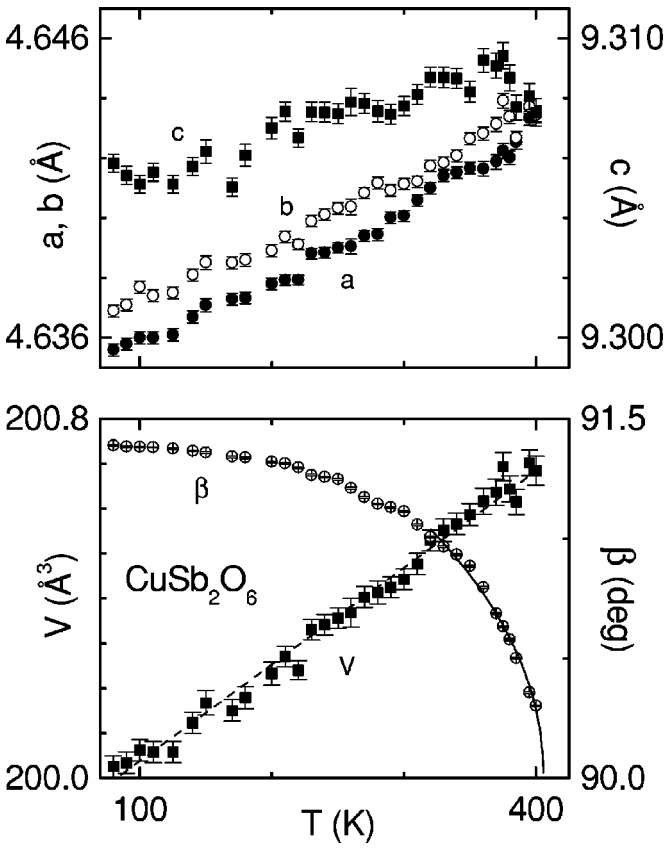

FIG. 2. The thermal expansion of the lattice parameters of $CuSb_2O_6$ in the temperature range $80 \leqslant T \leqslant 400$ K (upper panel) and the corresponding monoclinic angle and unit-cell volume (lower panel). The dashed line is guide to the eye.

II. SAMPLE PREPARATION AND CHARACTERIZATION

A. Crystal growth

For the preparation of polycrystalline $CuSb_2O_6$, mixed powders of CuO and Sb_2O_3 were ground and pressed into pellets. In the first step the sample was annealed in air at 950 °C for 12 h and in a second step refired at 1000 °C for 12 h after regrinding. The yellow color of the product is consistent with previous reports.[6,8]

The chemical vapor transport growth of $CuSb_2O_6$ single crystals with $TeCl_4$ as a transport agent is described in Ref. 4. In comparison with earlier flux-grown crystals which were strongly contaminated by vanadium from flux[2,10,11] the vapor technique results in purer crystals. Energy- and wavelength-dispersive x-ray (EDX and WDX) analyses detect neither tellurium nor chlorine contaminations in the crystals. Silicon, a possible contamination from the reactor walls, was also not evident in the crystals. The single-crystal sample under investigation which has the shape of a thin rectangular plate ($2 \times 3 \times 0.3$ mm^3) parallel to the (101) plane was cut from an as-grown crystal. Uniaxial pressure of 35 MPa was applied perpendicular to the plate in order to detwin the crystal. The x-ray reflections reveal, however, a slight remaining twinning.

B. X-ray diffraction

Temperature-dependent x-ray diffraction experiments were performed with increasing temperature at a STOE x-ray diffractometer working in a temperature range $80 < T < 400$ K by N_2-gas flow and confirmed the proper monoclinic structure of the polycrystalline material. The lattice parameters of $CuSb_2O_6$ at 300 K are $a = 4.6401(2)$ Å, $b = 4.6411(2)$ Å, $c = 9.3077(3)$ Å, and $\beta = 91.113(3)°$, in excellent agreement with the values reported in literature.[8,12]

Figure 2 shows the thermal expansion of the lattice parameters and the unit-cell volume for polycrystalline $CuSb_2O_6$ at temperatures $80 \leqslant T \leqslant 400$ K derived from Rietveld refinements of the Debye-Scherrer diffraction patterns. The unit-cell volume reveals a slight increase with increasing temperature. The behavior of a and b is similar. The lattice parameter c rises with half the slope of a and b and decreases slightly on approaching the phase transition. The monoclinic angle β decreases continuously with increasing temperature starting at 91.4° at 80 K and reaches nearly 90.0° at about 400 K. This indicates the expected monoclinic-to-tetragonal phase transition to take place

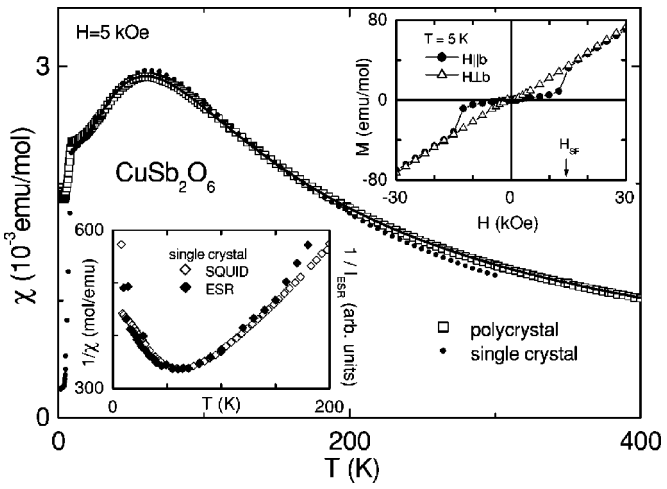

FIG. 3. Magnetic susceptibility vs temperature for $CuSb_2O_6$ at 5 kOe. Solid line: fit by the $S=1/2$ AF alternating-exchange Heisenberg chain model. Parameters are given in the text. Upper inset: magnetization of the single crystal vs applied field parallel and perpendicular to the b axis at 5 K. The spin-flop field H_{SF} is indicated by an arrow. Lower inset: inverse susceptibility and inverse ESR intensity of the single crystal vs temperature.

around this temperature. Due to its critical temperature behavior, the angle β may be taken as the order parameter of the phase transition. Fitting with the relation $\beta=90+c\cdot(1-T/T_{JT})^b$ in the temperature range closely below the phase transition (solid line in Fig. 2) yields a transition temperature $T_{JT}=406$ K and a critical exponent of $b=0.48$, which is close to 0.5 expected for the critical behavior of the primary order parameter in meanfield approximation.

C. Susceptibility

The temperature dependence $1.8<T<400$ K of the magnetization was measured in a commercial superconducting quantum interference device (SQUID) magnetometer (Quantum Design) at applied fields of 5 kOe. The magnetic susceptibility $\chi=M/H$ is plotted in Fig. 3. A broad maximum at about 60 K and an abrupt decrease at 8.5 K are observed for the polycrystalline sample. A comparison with the susceptibility of the single crystal, which is discussed together with specific heat in a separate paper,[4] proves the quality of the polycrystalline sample. The slight deviations for the single crystal above 200 K probably result from its anisotropy with respect to the direction of the applied magnetic field, which amounts approximately 10% at the susceptibility maximum between the a and c axes, but is averaged out in the polycrystalline sample. Additional deviations may arise from uncertainties due to its small mass (5 mg). Unlike the polycrystalline sample the single crystal was not heated above 300 K in order to avoid further twinning by crossing the phase transition at 400 K (see Sec. III).

The maximum value of the susceptibility χ_{max} at $T=60$ K is about 2.91×10^{-3} emu/mol. For $T>150$ K the susceptibility follows a Curie-Weiss law proportional $(T-\Theta)^{-1}$ with a negative Weiss constant of $\Theta=-65$ K, in agreement with the values reported in literature.[4,6,12] Below 150 K the susceptibility deviates considerably from the Curie-Weiss law as is expected for a quasi-one-dimensional antiferromagnet. To describe the observed temperature dependence, we used the $S=1/2$ antiferromagnetic alternating-exchange Heisenberg chain model.[13] In extension to the Bonner-Fisher approach this model allows for an alternation of the exchange constant of neighboring bonds and in some cases better describes the low-temperature regime $T\ll J/k_B$. The alternation parameter α denotes the ratio of the two antiferromagnetic exchange constants $0\leqslant J_2\leqslant J_1$. The fit for $11<T<400$ K describes the data perfectly (solid line in Fig. 3) and yields $J_1/k_B=93$ K, $g=2.22$, and $\alpha=1$. The results are in agreement with those given in Refs. 12 and 4 and demonstrate that no alternation exists in the one-dimensional chains of $CuSb_2O_6$.

Affirmation of the antiferromagnetic ordering of $CuSb_2O_6$ below 9 K is found in the upper inset of Fig. 3, where field-dependent magnetization measurements on the single crystal at 5 K are plotted. The curve for $H\|b$ shows two linear regimes with a transition region at about 12.5 kOe. This is characteristic for a spin-flop transition in an antiferromagnetically ordered phase with the field applied parallel to the easy axis. For $H\perp b$ the slope is unchanged throughout the entire field range. These results confirm the antiferromagnetic ordering of $CuSb_2O_6$ below 9 K with the easy antiferromagnetic axis along the b direction and agree with the magnetic structure reported by Ref. 5.

III. ELECTRON SPIN RESONANCE

The ESR measurements have been performed at a Bruker ELEXSYS E500-CW spectrometer at X-band (9.4 GHz) and Q-band (34 GHz) frequencies. The absorption spectra were obtained at constant microwave frequency dependent on the static magnetic field using a lock-in technique with field modulation, which yields the derivative of the resonance signal dP_{abs}/dH. In the temperature range 4.2–300 K (X band and Q band) continuous-flow He cryostats (Oxford Instruments) and above 300 K (only X band) a nitrogen cryostat (Bruker) were used. The powdered polycrystals were filled in quartz tubes and fixed in paraffin for measurements below room temperature or in NaCl at $300\leqslant T\leqslant500$ K. Measurements of the angular dependence of the ESR signal were carried out on the $CuSb_2O_6$ single crystal.

A. Spectra

The ESR spectra of the $CuSb_2O_6$ single crystal show four individual resonance lines of different intensity at different resonance fields. Only in the direction of the crystallographic b axis do they cumulate at the same resonance field. As we will discuss in detail below, this indicates the twinning of the crystal already observed in a Laue picture. The spectra are well fitted by four individual Lorentzian lines, each parametrized by its resonance field H_{res} and linewidth ΔH; only for orientations with resonances at about the same resonance field is the separation of the single lines difficult. Figure 4 gives examples for spectra at 20 K at different orientations

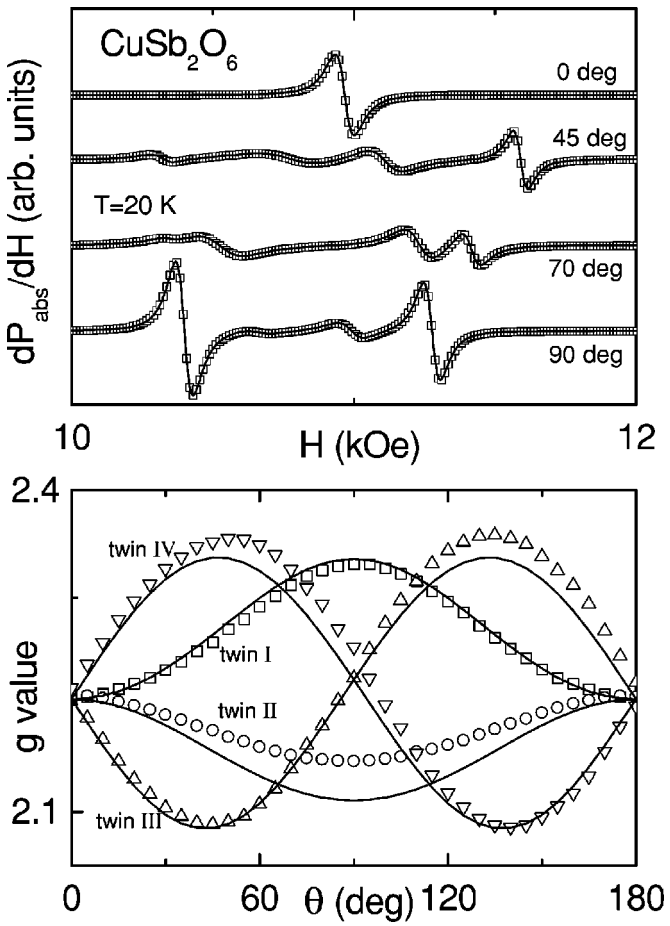

FIG. 4. Upper frame: ESR spectra of the $CuSb_2O_6$ single crystal (squares) at different orientations for the magnetic field applied within the (101) plane at 20 K. Solid lines: fit by four Lorentzian lines. Lower frame: angular dependence of the g factors of the four resonance lines. Solid lines: Simulation of the g values for the four possible twins, which are discussed in the text, with fixed molecular g factors: $g_{xx}=2.10$, $g_{yy}=2.06$, and $g_{zz}=2.46$.

for the external magnetic field applied within the (101) plane and shows the angular behavior of the four g factors ($g=h\nu/\mu_B H_{\rm res}$).

An orientation of the grains of the powder sample by the magnetic field was not possible. Therefore, the spectra of the powder (not shown here) consist of a mixture of resonances of the randomly oriented grains, revealing the typical powder pattern of an anisotropic g tensor, which can be approximated by three Lorentzian lines at $g_1=2.34$, $g_2=2.21$, and $g_3=2.11$ between 9 K and 200 K, in good agreement with the results of Giere *et al.*[8] Above 200 K the powder pattern merges to a single Lorentzian line with a g value of 2.22, which is slightly decreasing with increasing temperature and agrees with the average of the three low-temperature values and the value given in literature.[12] Due to the strong line broadening, it is not possible to get useful results at temperatures above 500 K, where the line cannot be distinguished from the background of the cavity anymore.

The integrated ESR intensity resembles the static susceptibility χ obtained from SQUID measurements and exhibits a maximum at about 60 K as well. Both inverse quantities of the single crystal are depicted in the lower inset of Fig. 3. At high temperatures the ESR intensity differs from the SQUID susceptibility because in this temperature range the condition $\Delta H \ll H_{\rm res}$ for their proportionality[14] is not valid due to the strong changes of the linewidth. However, a comparison with Gd_2BaCuO_5 (Gd^{3+}, $S=7/2$), which shows a similar broad resonance line, indicates that within an accuracy of 10% all Cu spins of $CuSb_2O_6$ powder and single crystal contribute to the paramagnetic resonance.

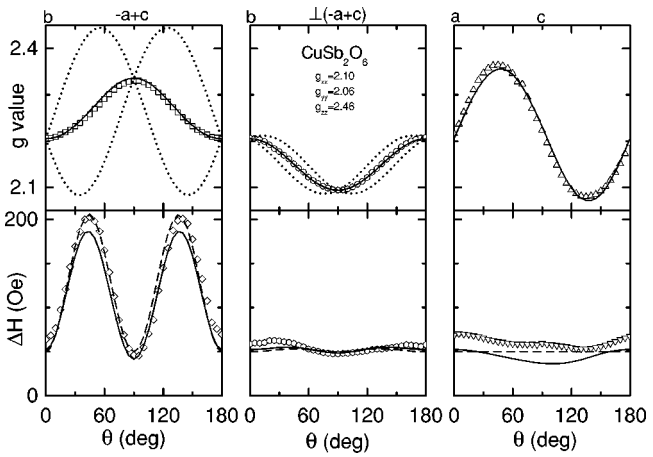

FIG. 5. Angular dependence of the g factor and linewidth of the $CuSb_2O_6$ single crystal with two elongated Cu-O2a bonds (twin I) at 20 K and 34 GHz. Upper panels: dotted lines denote individual g factors of the two inequivalent octahedra, solid lines the average of both. Lower panels: dashed lines from simulation of the linewidth with Eq. (3) and solid lines from simulation with Eq. (4) (see text).

B. Angular dependence

We investigated the angular dependence for three perpendicular crystallographic planes: first, the (101) plane [including the b direction and the $(-a+c)$ direction], second, the (010) ($\equiv ac$) plane, and, third, the plane perpendicular to both of them. Here, we confine our presentation to Q-band frequency (34 GHz) due to better resolution of the ESR spectra. Figure 5 shows the angular variation of the g factor and the linewidth of the most intense line at 20 K for the three different planes. It can be explained by the anisotropic Zeeman interaction due to the anisotropic g tensors of the two magnetically inequivalent Cu^{2+} ions in the elementary cell. Figure 1 illustrates the difference in the orientation of the g tensors of the two Cu places and gives local coordinates for them: $x_{1,2}$ and $y_{1,2}$ are positioned in the equatorial plane of an octahedron and $z_{1,2}$ is perpendicular to them. Therefore, the resonance line of a single crystal consists of two resonance signals at quite different magnetic fields $H_{\rm res}$, which merge to one resonance due to strong exchange coupling. For a given field direction the effective g factor of one octahedron is calculated by

$$g_{\rm eff,1,2}(\theta,\phi)=\sqrt{A^2+B^2+C^2}, \tag{1}$$

where

$$A = g_{aa}\sin\theta\cos\phi + g_{ba}\sin\theta\sin\phi + g_{ca}\cos\theta,$$

$$B = g_{ab}\sin\theta\cos\phi + g_{bb}\sin\theta\sin\phi + g_{cb}\cos\theta,$$

$$C = g_{ac}\sin\theta\cos\phi + g_{bc}\sin\theta\sin\phi + g_{cc}\cos\theta.$$

Here $g_{\alpha\beta}$ denote the components of the g tensor of one octahedron in crystallographic coordinates. Note that $g_{\alpha\beta}$ differ for the two inequivalent octahedra. Polar angle θ (with respect to c) and azimuth ϕ (with respect to a) give the orientation of the external field in the crystallographic system. The average of the effective g factors of both Cu places is observed by ESR. The dotted lines in Fig. 5 indicate the variation of the g factors of the two magnetically inequivalent chains; the solid line is the average of both simulated with molecular g factors $g_{xx}=2.10$, $g_{yy}=2.06$, and $g_{zz}=2.46$ of the octahedra and agrees nicely with the data. The g factors in the direction of the unit-cell coordinate system are $g_b=g_a=2.21$ and $g_c=2.23$.

In the case of sufficient exchange narrowing of the averaged signal, the corresponding linewidth due to the anisotropic Zeeman interaction is proportional to the square of the difference of the two inequivalent g tensors $(\Delta g)^2$. In high-temperature approximation ($T \gg J^{\text{inter}}/k_B$) it can be expressed as[15]

$$\Delta H_{AZ}(\text{kOe}) \approx \frac{g\mu_B H_0^2}{|J|}\left(\frac{\Delta g}{g}\right)^2 \approx 6.7\frac{g[H_0(10^4\ \text{Oe})]^2}{J^{\text{inter}}(\text{K})}\left(\frac{\Delta g}{g}\right)^2. \quad (2)$$

Note that for the anisotropic Zeeman interaction the interchain exchange $J^{\text{inter}}=0.03J$ (Ref. 4) is responsible for the narrowing, because the octahedra within one chain have all the same orientation in the crystal lattice. Therefore, the high-temperature approximation can be used even at 20 K. At Q-band frequency with a resonance field of about 12 kOe and with $J/k_B=93$ K and $\Delta g=0.4$ we obtain $\Delta H_{AZ} \approx 138$ Oe. This is in very good agreement with the amplitude of the linewidth modulation in the (101) plane, where we observe the strongest difference between the molecular g values. The dashed lines in Fig. 5 are generated by the equation

$$\Delta H_{\text{sim}} = 1400\ \text{Oe} \times (\Delta g)^2 + 50\ \text{Oe} \quad (3)$$

and fit rather well the observed linewidth. Since the two g tensors are symmetric with respect to the ac plane, Δg vanishes by rotation in this plane and the linewidth should remain constant.

The remaining three lines of the ESR spectrum are due to two equivalent alternatives of the elongation of the oxygen octahedra—namely, along the Cu-O2a or Cu-O2 bond; i.e., there are four possibilities to arrange the two different elongated CuO_6 polyhedra in the monoclinic unit cell, resulting in the tendency to form twinned single crystals. The line with about half of the intensity of the highest one (twin I, elongated Cu-O2a bonds) belongs to a part of the crystal (twin II), in which the Cu-O2 bonds of both oxygen octahedra are elongated and consequently their local coordinate systems have to be rotated by about 90° around the x_i axis, so that z_i still points along the elongated Cu-O bond (see Fig. 1). The angular dependence of the g factor and the linewidth are similar to that in Fig. 5 and a simulation with the same values for g_{xx}, g_{yy}, and g_{zz} follows the run of the data. The two lines with low intensity are due to small domains, in which different axes of the two inequivalent octahedra are stretched: In twin III octahedron 1 (coordinates x_1, y_1, z_1) possesses an elongated Cu-O2a bond and octahedron 2 (coordinates x_2, y_2, z_2, to be rotated) an elongated Cu-O2 bond; in twin IV it is reversed. A simulation for twin III using the same g values as above results in an angular dependence of the g factor shown in Fig. 6 together with the corresponding data. Again the dotted lines indicate the behavior of the g values of the single octahedra, the solid line the average of both. The angular variation of the weak lines is described sufficiently. Also in this case the calculation of the expected linewidth with Eq. (3) reproduces the observed linewidth (dashed lines in Fig. 6). Figure 4 (lower frame) clarifies the quality of the simulations with fixed values for the molecular g factors: The corresponding data of the four lines observed with the external magnetic field applied within the (101) plane possess the same angular dependences as the simulations.

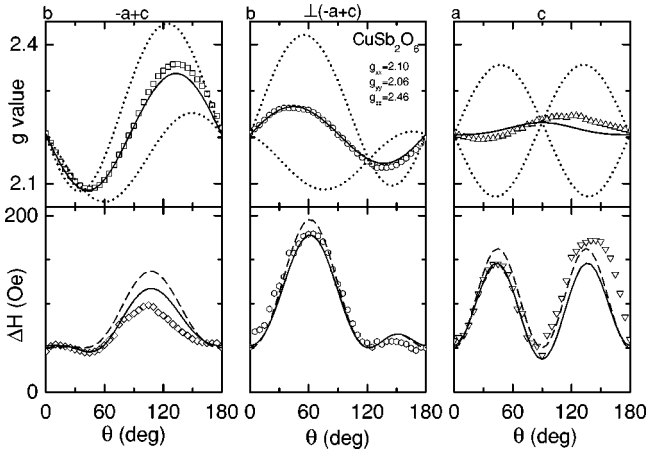

FIG. 6. Angular dependence of the g factor and linewidth of the $CuSb_2O_6$ single crystal with an elongated Cu-O2a bond and an elongated Cu-O2 bond (twin III) at 20 K and 34 GHz. Upper panels: dotted lines denote individual g factors of the two inequivalent octahedra, solid lines the average of both. Lower panels: dashed lines from simulation of the linewidth with Eq. (3) and solid lines from simulation with Eq. (4) (see text).

For simulating the angular dependence of the linewidth we had to add a constant of 50 Oe in Eq. (3), which probably is caused by the symmetric anisotropic exchange interaction similar as in other Cu chain systems like $LiCuVO_4$.[16] This anisotropic exchange interaction itself possesses an angular dependence, and we refined our former expression by replacing the constant with the average of the contributions of the two inequivalent chains to the linewidth ΔH_1 and ΔH_2 due to the anisotropic exchange:

$$\Delta H_{\text{sim,AE}} = 1400\ \text{Oe} \times (\Delta g)^2 + \frac{\Delta H_1 + \Delta H_2}{2}. \quad (4)$$

We considered two contributions: the anisotropic exchange interaction $J^i_{\alpha\beta}$ ($i=1,2$ denotes inequivalent chains) between the copper spins within one chain and the exchange interaction $J^{\text{inter}}_{\alpha\beta}$ between neighboring Cu chains in the ab plane (interchain). So for a single chain the ESR linewidth is determined by[17]

$$\Delta H_i = \frac{\hbar}{g\mu_B} \frac{M_2(J^i_{\alpha\beta}) + M_2(J^{\text{inter}}_{\alpha\beta})}{\omega_{\text{ex}}}, \tag{5}$$

with the Planck constant $\hbar$, the Bohr magneton μ_B, the second moments M_2 due to the respective anisotropic exchange contributions, and the exchange frequency $\omega_{\text{ex}} \approx J/\hbar$. Equation (5) is exact only in the high-temperature approximation $J \ll k_B T$. However, according to recent theoretical calculations on ESR in low-dimensional systems by Oshikawa and Affleck[18] this expression still describes the angular dependence at temperatures $k_B T < J$, if the ESR linewidth is dominated by a single type of anisotropic interaction only. So Eq. (4) can be used to simulate our data, but the exact temperature dependence is unknown and therefore only the relative values of the anisotropic exchange components are of relevance, except for $k_B T \gg J$.

For calculating the linewidths ΔH_1 and ΔH_2 we used the same procedure as described in Ref. 16. The tensors $J^i_{\alpha\beta}$ have to be treated like the g tensors, because they are diagonal in the local coordinate systems of the oxygen octahedra (x_i, y_i, z_i), whereas the tensor $J^{\text{inter}}_{\alpha\beta}$ is diagonal in the crystallographic coordinate system (a,b,c). The best results are obtained with relative diagonal exchange tensor components $J^i_{zz}/J^i_{xx} = -3$, $J^i_{yy}/J^i_{xx} = 2$, $J^{\text{inter}}_{aa}/J^{\text{inter}}_{bb} = -1$, and $J^{\text{inter}}_{cc}/J^{\text{inter}}_{bb} = 0$ and are indicated as solid lines in the lower panels of Figs. 5 and 6. Deviations are due to a slight misorientation of the crystal with respect to the external magnetic field during the rotation and the disregard of other contributions which may become important at low temperatures. Nevertheless, taking into account the symmetric anisotropic exchange interaction, at least, enhances the quality of the simulations of the linewidth.

Finally we shortly comment on the magnitude of anisotropic exchange interaction, which dominates the relaxation in other linear-chain compounds: Below 200 K (only the static Jahn-Teller effect; see Sec. III C) but clearly above $T = J/k_B$ the linewidth contribution caused by the anisotropic exchange is by far smaller than the expected value of 1 kOe from standard estimation following Ref. 15. However, such estimates do not take into account details of the bond structure in the chains. In the case of a ring geometry of the Cu-O bonds like in $LiCuVO_4$,[16] it was shown to be strongly enhanced. In the present compound the longer path via two subsequent oxygen ions may weaken the anisotropic exchange integrals.

C. Temperature dependence

The $CuSb_2O_6$ single-crystal and polycrystalline samples were examined at X-band frequency between 4 and 330 K; for higher temperatures exclusively the polycrystalline sample was used in order to avoid further twinning of the single crystal due to crossing the phase transition. The temperature dependence of the linewidth and of the g value of the single crystal was investigated in the b, $(-a+c)$ and perpendicular to the $(-a+c)$ direction by considering only the most intense line of the spectra (twin I). No signal exists for temperatures below 9 K due to the antiferromagnetic ordering, but an ESR signal due to the spin-flop transition is detected at a magnetic field of about 1.25 T in the b direction, which vanishes at the transition temperature and agrees with the results of the magnetization measurements (see above). Figure 7 shows the temperature-dependent behavior of the linewidth and the g factors for both the single-crystal and powder samples. We can clearly identify three temperature regimes.

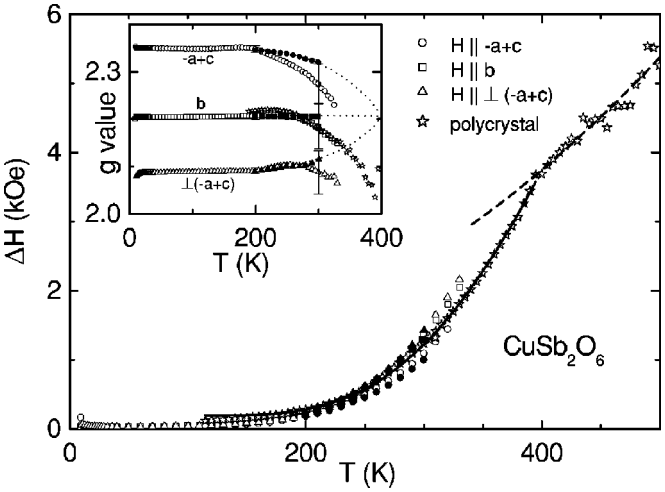

FIG. 7. Temperature dependence of the ESR linewidth ΔH for three orientations of the $CuSb_2O_6$ single crystal in the external magnetic field [along b, $(-a+c)$, and $\perp(-a+c)$] as well as for the polycrystal. Solid line: fit with exponential activation law. Dashed line: fit with Eq. (6). Inset: temperature dependence of the g factors of the polycrystal and single crystal. Open symbols: X-band measurement. Note the different error bars. Solid symbols: Q-band measurement. Dotted lines: expected behavior.

(i) Below 200 K the g factors remain constant. The linewidth increases monotonously on increasing the temperature starting at a minimum value of ≈ 25 Oe at about 30 K. Below $T = 30$ K the resonance line broadens on approaching the magnetic order at 9 K. For $H \| (-a+c)$ the linewidth is smallest over the whole temperature range.

(ii) Between 200 K and 400 K the anisotropy of the g value gradually diminishes with increasing temperature. At the same time the linewidth increases strongly up to 3.5 kOe at 400 K. For this reason the determination of the g value becomes more and more imprecise. We had strong doubts about the additional shifts observed in our X-band data above 200 K, which probably are caused by the strong increase of the linewidth. So we checked the results by Q-band measurements with better resolution (closed symbols in Fig. 7), which affirm our assumption and indicate the approach of an average g value at 400 K. The behavior of the g values is very similar to that in $[Cu^{II}(TACN)_2]Cu^{I}(CN)_3$, where also a transition from static to dynamic Jahn-Teller effect is observed.[19] Already in the static regime over a wide tempera-

ture range below the transition temperature the g tensor exhibits a gradual motional narrowing for both compounds, finally approaching the average value in the dynamic regime. Dotted lines in the inset of Fig. 7 indicate the expected behavior of averaging. In the high-temperature phase a dynamic change between the different distortion possibilities of the oxygen octahedra takes place. An equilibration between the two conform elongations of the oxygen octahedra occurs and results in time-averaged compressed octahedra.[20] This temperature dependence of the distortion of the octahedra and thereby the change of the monoclinic angle β is nicely reflected by the g factors.

In Fig. 7 the linewidth of the polycrystal is included above 200 K, where its signal can be well described by a single Lorentzian line. Below 250 K the linewidth of the polycrystal is larger than that of the single crystal due to the superposition of different lines at different resonance fields. However, at higher temperatures the linewidth becomes large compared to the decreasing anisotropy of the resonance field and, hence, the polycrystalline data resemble the average of the single-crystal linewidth.

(iii) At the phase transition at 400 K the linewidth exhibits a distinct kink. Finally, in the tetragonal phase, the data increase further, but with a reduced slope.

At Q-band frequency our accessible temperature range is confined to $T<300$ K, where the observed changes of the linewidth are comparable to the X-band results. As the strong effects in the linewidth become crucial only above room temperature, we will concentrate in the following discussion on our results at 9.4 GHz.

To discuss the linewidth we start in the high-temperature phase. Here the linewidth of 5 kOe is by far larger than in other linear-chain compounds like $CuGeO_3$ (Ref. 15) or $LiCuVO_4$ (Ref. 16). In those compounds the Jahn-Teller effect remains static and the linewidth can be explained by pure spin-spin relaxation only, where the main contribution results from the symmetric anisotropic exchange interaction and exhibits saturation behavior at temperatures $T \gg J/k_B$. In contrast the linewidth in $CuSb_2O_6$ shows no indication of saturation up to 500 K. As we deal here with the dynamic Jahn-Teller regime, we suggest that the relaxation process via phonons is dominant. Such a situation was described by Ineev and Kochelaev[21] for a two-dimensional case and may be valid for $CuSb_2O_6$ due to the square planar Cu^{2+} lattice of the trirutil structure, especially because only the asymptotic high-temperature behavior is considered. In this context the relaxation rate Γ caused by the dynamic Dzyaloshinski-Moriya interactions appearing due to the Q_4, Q_5 vibration modes of the octahedra is described by

$$\frac{g\mu_B}{\hbar}\Delta H = \Gamma = 7.6\pi^3\left(\frac{\lambda G}{\Delta^2}\right)^2 \frac{\hbar\Omega}{J}\frac{\hbar}{md^2}\coth^2\left(\frac{\hbar\Omega}{2k_BT}\right), \tag{6}$$

with the spin-orbit coupling λ, the cubic crystal-field splitting Δ, the orbital-lattice coupling $G \approx 2\Delta$, and the vibration frequency Ω. Moreover, the exchange integral $J/k_B = 93$ K, the oxygen mass $m = 16u$, and the size $d = 4$ Å of the octahedron were used. The dashed line in Fig. 7 denotes the fit to the data by Eq. (6) for $T > 400$ K with effectively two fit parameters: It yields $\Omega = 10.7$ THz for the vibration frequency of the octahedra typical for optical phonons. The factor $(\lambda G/\Delta^2)$ results in ≈ 0.026, which is admittedly smaller than expected.[14] However, this is probably caused by the uncertainty of the assumption about G and the result is still the right order of magnitude for the spin-orbit coupling.

Approaching the phase transition from below the high-temperature relaxation mechanism seems to be thermally activated. Between 200 K and 400 K we tried to describe the linewidth by the expression

$$\Delta H = \Delta H_0 + A\exp\left(-\frac{2\Delta}{T}\right). \tag{7}$$

The prefactor A corresponds to Eq. (6), but for simplicity we neglected its temperature dependence, which varies only slowly compared to the exponential factor near the phase transition. Figure 7 shows good coincidence of fit and data with $\Delta = 742$ K and $\Delta H_0 = 195$ Oe. The residual linewidth ΔH_0 is consistent with the low-temperature linewidth dominated by the anisotropic Zeeman interaction as discussed in the paragraph of the angular dependence. It is interesting to consider the relation between the energy gap Δ and the transition temperature T_{JT}, which yields $2\Delta/T_{JT} = 3.7(2)$. This is close to the value of 3.5 predicted by mean-field theory for a second-order phase transition. Moreover, the Jahn-Teller energy E_{JT} is related to the ^2E_g ground-state splitting by $\Delta E = 4E_{JT}$.[20] The ground-state splitting was observed in Ref. 8 and leads to $E_{JT} = 770$ K in good agreement with our energy gap Δ.

This can be understood in the following way: Approaching the phase transition near 400 K the dynamic Jahn-Teller effect is activated as we already discussed with respect to the monoclinic angle and the g value. Some octahedra dispose already enough thermal energy to change the direction of elongation temporary and to override the existing energy gap Δ of the ground-state potential surface, caused by higher-order Jahn-Teller coupling terms and strains induced by packing effects,[8,20] whereby they contribute to the relaxation.

We have to mention that the mean-field theory implies a temperature dependence of the energy gap $\Delta(T) = \Delta_0(1 - T/T_{JT})^b$ with $b = 0.5$. Fitting with this temperature-dependent gap yields the best result for $\Delta_0 = 635$ K, $T_{JT} = 395$ K, $b = 0.9$, and $\Delta H_0 = 142$ Oe. The fit curve nearly coincides with the curve for the temperature-independent gap. Again $2\Delta_0/T_{JT} = 3.2$ agrees quite well with the theoretical expectation. Only the exponent b is larger than predicted. For a deeper analysis of this result further theoretical investigations are necessary.

IV. CONCLUSION

To summarize, we presented detailed x-ray, magnetization, and ESR investigations on $CuSb_2O_6$ polycrystals and single crystals. The low-dimensional magnetic behavior is corroborated by the maximum around 60 K in the temperature dependence of the integrated ESR intensity as well as in the static susceptibility χ obtained from SQUID measure-

ments. χ(T) can be perfectly described as a uniform $S=1/2$ antiferromagnetic Heisenberg chain with an antiferromagnetic exchange integral of about $J/k_B=93$ K. A spin-flop transition observed by ESR and magnetization measurements confirms the antiferromagnetic ordering of $CuSb_2O_6$ below 9 K.

Angular-dependent ESR measurements on a $CuSb_2O_6$ single crystal revealed a fourfold twinning of the sample. The behavior of the g factor and the linewidth of each twin can be explained by the anisotropic Zeeman interaction, taking into consideration the existence of two magnetically inequivalent oxygen octahedra and the different possibilities for the elongation of one axis of the octahedra. Taking into account the anisotropic exchange interaction the description of the corresponding linewidth could be improved.

The activation of the dynamic Jahn-Teller effect was shown to account for the strong increase of the linewidth with temperature approaching the monoclinic-to-tetragonal phase transition at about 400 K and a Jahn-Teller energy of $E_{JT}=742$ K was received, in excellent agreement with optical investigations from literature.

For a complete analysis of the temperature dependence of the linewidth further theoretical effort is necessary. Particularly, the connection of the monoclinic angle β related to the order parameter and the energy gap $\Delta=\Delta E_{JT}$ is of interest.

ACKNOWLEDGMENTS

We are grateful to D. Vieweg, M. Müller, and A. Pimenova for sample preparation and SQUID and x-ray characterization. This work was supported by the German Bundesministerium für Bildung und Forschung (BMBF) under Contract No. VDI/EKM 13N6917, by the program Universities of Russia (Grant No. 01.01.023), and partly by the Deutsche Forschungsgemeinschaft (DFG) via the Sonderforschungsbereich (SFB) 484 and the joint project with the Russian Foundation for Basic Research (RFBR) under Contract No. 436RUS113/628. The work of A.V.P. and W.A. was supported by the Deutsche Forschungsgemeinschaft (DFG) in the framework of the Schwerpunktprogramm 1073 and the work of A.D.I. was supported by CRDF via Grant No. REC-007.

[1] M. Hase, I. Terasaki, and K. Uchinokura, Phys. Rev. Lett. **70**, 3651 (1993).
[2] A. Nakua and J. E. Greedan, J. Solid State Chem. **118**, 199 (1995).
[3] M. Kato, A. Hatazaki, K. Yoshimura, and K. Kosuge, Physica B **281&282**, 663 (2000).
[4] A. V. Prokofiev, F. Ritter, W. Assmus, B. J. Gibson, and R. K. Kremer, J. Cryst. Growth **247**, 457 (2003).
[5] M. Kato, T. Ishii, K. Kajimoto, K. Yoshimura, K. Kosuge, M. Nishi, and K. Kakurai, J. Phys. Chem. Solids **63**, 1129 (2002).
[6] A. Nakua, H. Yun, J. N. Reimers, J. E. Greedan, and C. V. Stager, J. Solid State Chem. **91**, 105 (1991).
[7] J. D. Donaldson, A. Kjekshus, D. G. Nicholson, and T. Rakke, Acta Chem. Scand., Ser. A **29**, 803 (1975).
[8] E.-O. Giere, A. Brahimi, H. J. Deiseroth, and D. Reinen, J. Solid State Chem. **131**, 263 (1997).
[9] H.-J. Koo and M.-H. Whangbo, J. Solid State Chem. **156**, 110 (2001).
[10] S. Shimada, K. Kodaira, and T. Matsushita, J. Cryst. Growth **72**, 753 (1985).
[11] A. M. Nakua and J. E. Greedan, J. Cryst. Growth **154**, 334 (1995).
[12] M. Yamaguchi, T. Furuta, and M. Ishikawa, J. Phys. Soc. Jpn. **65**, 2998 (1996).
[13] D. C. Johnston, R. K. Kremer, M. Troyer, X. Wang, A. Klümper, S. L. Budko, A. F. Panchula, and P. C. Canfield, Phys. Rev. B **61**, 9558 (2000).
[14] A. AbragamandB. Bleaney, *Electron Paramagnetic Resonance of Transition Ions* (Clarendon Press, Oxford, 1970).
[15] B. Pilawa, J. Phys.: Condens. Matter **9**, 3779 (1997).
[16] H.-A. Krug von Nidda, L. E. Svistov, M. V. Eremin, R. M. Eremina, A. Loidl, V. Kataev, A. Validov, A. Prokofiev, and W. Assmus, Phys. Rev. B **65**, 134445 (2002).
[17] R. Kubo and K. Tomita, J. Phys. Soc. Jpn. **9**, 888 (1954).
[18] M. Oshikawa and I. Affleck, Phys. Rev. B **65**, 134410 (2002).
[19] P. Chaudhuri, K. Oder, K. Wieghardt, J. Weiss, J. Reedijk, W. Hinrichs, J. Wood, A. Ozarowski, H. Stratemaier, and D. Reinen, Inorg. Chem. **25**, 2951 (1986).
[20] D. Reinen and M. Atanasov, Magn. Reson. Rev. **15**, 167 (1991).
[21] A. D. Ineev and B. I. Kochelaev (unpublished).